Recycling cavity gain

Issue 1

I. Nardecchia[1,2]

[1]Università degli Studi di Roma Tor Vergata, I-00133 Roma, Italy
[2]INFN, Sezione di Roma Tor Vergata, I-00133 Roma, Italy

June 6, 2017

Contents

1 Introduction

The goal of this document is to derive the sideband recycling cavity gain equations in order to estimate it from the interferometer signals. The recycling gain is one of the most significant figures of merit to evaluate the entity of aberrations and assess the stability of the Power Recycling Cavity (*PRC*). Once the interferometer sensitivity to the optical aberrations has been investigated the best thermal compensation strategy can be defined.
In the first part the main fields inside an optical system have been described starting from the simple Fabry-Pérot (*FP*) cavity to a power recyled interferometer (*ITF*). Since we are interested in the evaluation of the recycling cavity gain only the calculations for the beam reflected by the interferometer towards the symmetric port have been developed both in the recombined and in the recycled configurations. In the second part the equations to evaluate the sidebands cavity gains have been derived and then applied to the latest AdV data to check the consistency of the model.

2 Fields Equations

2.1 Fabry-Pérot cavity

The fields circulating in a simple Fabry-Pérot cavity are shown in Fig. 1. The input and end mirrors are labelled by numbers 1 and 2 and their distance is defined by L.

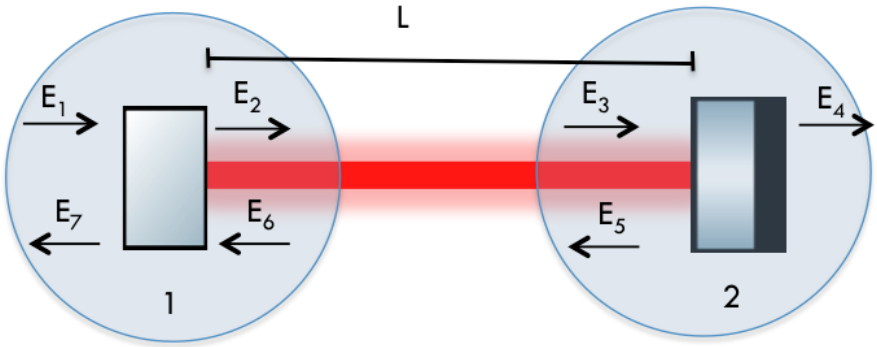

Figure 1: *Scheme of a Fabry-Pérot resonant cavity with the field and length definitions as used in the calculations.*

It can be demonstrated that the reflected field E_7 can be written as [1]:

$$E_7 = i\frac{r_1 + r_2(1-L_1)e^{2ikL}}{1 + r_1 r_2 e^{2ikL}}E_1, \tag{1}$$

where r_1 and r_2 are the reflectivity of input and end mirrors, and L_1 are the losses of the input mirror.
For the standard *Frontal Modulation Technique* only the carrier resonates inside the Fabry-Pérot cavity while the sidebands are anti-resonant in the arm cavities [2]. At the anti-resonance condition ($e^{2ikL} = 1$):

$$r_{anti} = i\frac{r_1 + r_2(1-L_1)}{1 + r_1 r_2} = i\rho_{anti} \sim i. \tag{2}$$

By imposing the resonance condition ($e^{2ikL} = -1$) the reflectivity coefficient for the carrier is:

$$r_{res} = i\frac{r_1 - r_2(1 - L_1)}{1 - r_1 r_2}. \tag{3}$$

By introducing the *finesse* ($\mathcal{F}$) and the round trip losses RTL of the Fabry-Pérot cavity one can write [4]:

$$r_{res} \sim -i(1 - \frac{\mathcal{F}}{\pi}RTL) = -i\rho_{res}. \tag{4}$$

In Advanced Virgo $\mathcal{F} \sim 450$ and $RTL = 75$ ppm, so $\rho_{res} = 0.9893$ [6].

2.2 Simple Michelson Interferometer

The simple Michelson interferometer is composed by the beam splitter and two equivalent mirrors formed by the two Fabry-Pérot cavities with reflectivity r_{res} (eq. 4) and r_{anti} (eq. 2) for the carrier and sidebands respectively (Fig. 2). The power recycling mirror (PR) has also been considered in the calculations but it is misaligned to not form the power recycling cavity. This configuration is also defined *recombined configuration* (rec). The transmission and reflection coefficients of the power recycling mirror are denoted by t_{PR} and r_{PR} and in Advanced Virgo they are equal to $t_{PR} = \sqrt{0.04835} = 0.2198$ and $r_{PR} = \sqrt{1 - 0.04835} = 0.9755$ [3].

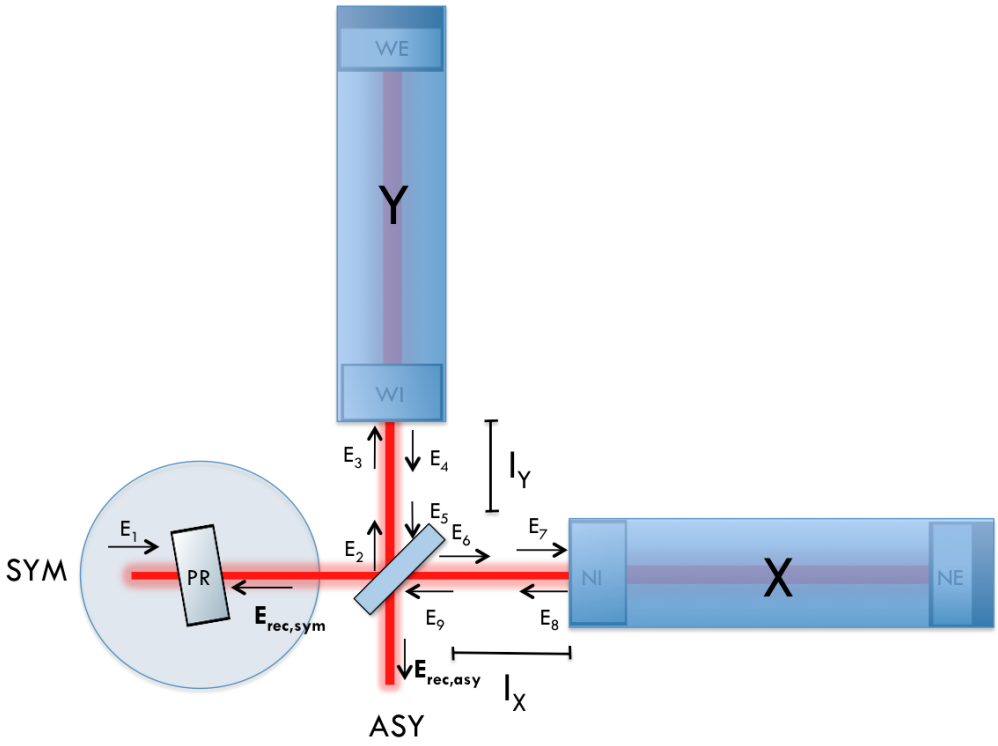

Figure 2: *Scheme of a simple Michelson Interferometer with the field and length definitions as used in the calculations. The power recycling mirror is shown but it is misaligned to not form another resonant cavity.*

The reflection towards the input laser is called symmetric port (sym), while the recombination at the beam splitter is called anti-symmetric port (asy). The two arms are called X and Y and the distances between the beam splitter and the input arm mirrors are labelled by l_X and l_Y

respectively.
Let's introduce two more useful definitions of lengths:

$$l_+ = \frac{l_X + l_Y}{2} \quad \text{and} \quad l_- = \frac{l_X - l_Y}{2}. \tag{5}$$

The fields, $E_{rec,sym}$ and $E_{rec,asy}$, for the symmetric and anti-symmetric ports respectively, are [1]:

$$E^{Car}_{rec,sym} = it_{PR} r_{res} e^{i2kl_+} \sin(2kl_-) E_1, \tag{6}$$

$$E^{Car}_{rec,asy} = it_{PR} r_{res} e^{i2kl_+} \cos(2kl_-) E_1. \tag{7}$$

Usually the Michelson differential length is tuned in order to have destructive interference for the carrier at the anti-symmetric port. This is equivalent to impose:

$$\cos(2kl_-) = 0, \tag{8}$$

therefore:

$$2kl_- = \pi N + \frac{\pi}{2} \rightarrow l_- = \frac{\lambda}{8} + N\frac{\lambda}{4}, \tag{9}$$

where N is any integer and λ is the laser wavelength.
This condition for l_- is called the *locking condition* of the Michelson interferometer on the carrier at the dark fringe. As a consequence the power at the symmetric port is maximum. The presence of the macroscopic difference between the length of the two arms, the so called *Schnupp asymmetry* defined as:

$$\Delta L = l_X - l_Y = N\lambda; \tag{10}$$

makes it possible to have simultaneously the carrier reflected to the symmetric port and a small fraction of the sidebands leaking to the anti-symmetric port as is shown below in eqs. 14-15. In Advanced Virgo $\Delta L = 0.23$ m.
From now on only the symmetric port will be considered in the calculations.
Considering $\Omega = 2\pi f_{mod}$ where f_{mod} is the modulation frequency, and replacing $k \rightarrow k' = k \pm \frac{\Omega}{c}$ into eq. 6, the reflected field for the sidebands $E^{Sid}_{rec,sym}$ modulated at $\pm f_{mod}$ at the symmetric port can be derived to be [1]:

$$E^{Sid}_{rec,sym} = it_{PR} r_{anti} e^{i2kl_+} e^{\pm i2\frac{\Omega}{c} l_+} \sin\left(2kl_- \pm \frac{\Omega \Delta L}{c}\right) E_1, \tag{11}$$

having considered $\sin\left(2kl_- \pm \frac{2\Omega}{c} l_-\right) = \sin\left(2kl_- \pm \frac{\Omega \Delta L}{c}\right)$.
The term $e^{\pm i2\frac{\Omega}{c} l_+}$ is due to the difference of the wave number k of the sideband with respect to that of the carrier [1].

Considering eq. 6, the carrier field reflection coefficient at the symmetric port is:

$$r^{Car}_{sym} = e^{i2kl_+} \rho_{res} \sin(2kl_-), \tag{12}$$

and for the sidebands (eq. 11) the coefficient is:

$$r^{Sid}_{sym} = -e^{i2kl_+} e^{\pm i2\frac{\Omega}{c} l_+} \sin\left(2kl_- \pm \frac{\Omega \Delta L}{c}\right), \tag{13}$$

having considered eqs. 2-4.

It is also useful to define the following quantities:

$$R_{sym}^{Car} = |\rho_{res} \sin(2kl_-)|^2, \tag{14}$$

$$R_{sym}^{Sid} = \left| \sin\left(2kl_- \pm \frac{\Omega\Delta L}{c}\right)\right|^2. \tag{15}$$

The term $|\sin(2kl_-)|^2$ can be also written as [5]:

$$|\sin(2kl_-)|^2 = 1 - MICH, \tag{16}$$

where $MICH$ is the dark fringe offset defined as the ratio between the power at the anti-symmetric port and the sum of the powers at symmetric and anti-symmetric ports, i.e. $\frac{P_{asy}}{P_{asy}+P_{sym}}$ [7]. By replacing eq. 16 into eqs. 14-15 one obtains:

$$R_{sym}^{Car} = \rho_{res}^2(1 - MICH), \tag{17}$$

$$\begin{aligned} R_{sym}^{SidUp} =& (1 - MICH)\cos^2\left(\frac{\Omega\Delta L}{c}\right) + MICH \sin^2\left(\frac{\Omega\Delta L}{c}\right) + \\ &+ 2\sqrt{1 - MICH} \times MICH \times \cos\left(\frac{\Omega\Delta L}{c}\right)\sin\left(\frac{\Omega\Delta L}{c}\right), \end{aligned} \tag{18}$$

$$\begin{aligned} R_{sym}^{SidLow} =& (1 - MICH)\cos^2\left(\frac{\Omega\Delta L}{c}\right) + MICH \sin^2\left(\frac{\Omega\Delta L}{c}\right) - \\ &- 2\sqrt{1 - MICH} \times MICH \times \cos\left(\frac{\Omega\Delta L}{c}\right)\sin\left(\frac{\Omega\Delta L}{c}\right), \end{aligned} \tag{19}$$

where eq. 17 is the reflectivity of Michelson for the carrier, eq. 18 for the upper sideband ($SidUp$) and eq. 19 for the lower one ($SidLow$).
At the dark fringe ($MICH = 0$) eqs. 14-15 (or eqs. 17 and 18-19) become:

$$R_{sym}^{Car} = \rho_{res}^2, \tag{20}$$

$$R_{sym}^{Sid} = \left| \cos\left(\frac{\Omega\Delta L}{c}\right)\right|^2. \tag{21}$$

The reflectivities of the simple Michelson interferometer for the sidebands at the modulation frequencies f_{mod} adopted in Advanced Virgo [6] are summarized in Tab. 1.

From eq. 6 and eq. 11 for carrier and sidebands respectively, the power transmitted back toward the laser by the PR mirror is:

$$|E_{rec,sym}^{Car}|^2 = \rho_{res}^2 |\sin(2kl_-)|_{rec}^2 T_{PR} |E_1|^2, \tag{22}$$

$$|E_{rec,sym}^{Sid}|^2 = \left| \sin\left(2kl_- \pm \frac{\Omega\Delta L}{c}\right)\right|_{rec}^2 T_{PR} |E_1|^2, \tag{23}$$

where $T_{PR} = t_{PR}^2$.

f_{mod} [MHz]	R^{Sid}_{sym}
6.270777	0.99909
56.43699	0.92780
119.1447	0.70485

Table 1: The reflectivities of the Michelson interferometer for the sidebands at the different modulation frequencies adopted in Advanced Virgo.

2.3 Power-Recycled interferometer

A power recycled interferometer (*recy*) is obtained by aligning the power recycling mirror and tuning the distance PR-BS in order to obtain another resonant cavity (Fig. 3).

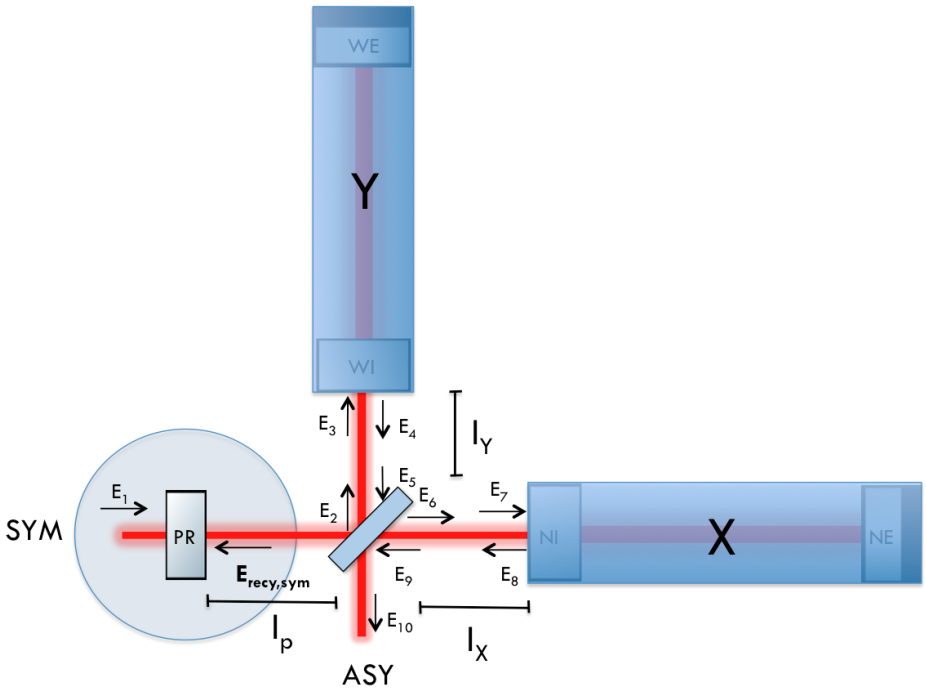

Figure 3: *Scheme of a Michelson interferometers with the power recycling mirror aligned (recycled state).*

The Michelson part can be treated as a single optical object with the reflection coefficients for carrier and sideband computed in eqs. 12-13 (Fig. 4). The reflected fields, $E^{Car}_{recy,sym}$ and $E^{Sid}_{recy,sym}$, at the symmetric port are respectively [1]:

$$E^{Car}_{recy,sym} = \frac{\sqrt{1-L_{PRC}}t_{PR}r^{Car}_{sym}e^{i2kl_p}}{1-ir_{PR}r^{Car}_{Sym}\sqrt{1-L_{PRC}}e^{i2kl_p}}E_1, \tag{24}$$

$$E^{Sid}_{recy,sym} = \frac{\sqrt{1-L_{PRC}}t_{PR}r^{Sid}_{sym}e^{i2kl_p}e^{\pm i2\frac{\Omega}{c}l_p}}{1-ir_{PR}r^{Sid}_{Sym}\sqrt{1-L_{PRC}}e^{\pm i2\frac{\Omega}{c}l_p}e^{i2kl_p}}E_1, \tag{25}$$

where l_p is the distance between the PR and the BS and L_{PRC} are the round trip losses inside the recycling cavity.
The resonance condition for the carrier in the power recycling cavity is:

$$e^{2ik(l_++l_p)} = e^{2ikl_{PRC}} = -i, \tag{26}$$

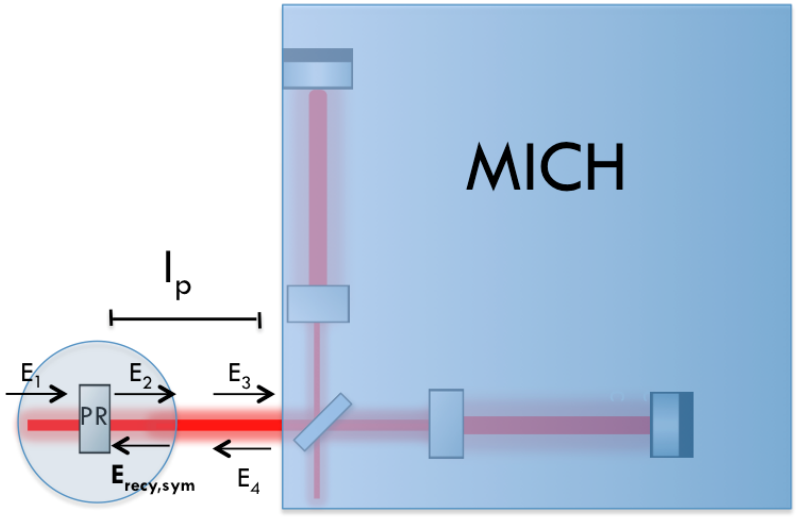

Figure 4: *Scheme of a Power-Recycled Michelson interferometers.*

while for the sideband another additional condition has to be fulfilled:

$$e^{\pm i2\frac{\Omega}{c}(l_p+l_+)} = e^{\pm 2i\frac{\Omega}{c}l_{PRC}} = -1. \tag{27}$$

By replacing eqs. 12-13 in eqs. 24-25 and applying the two resonant conditions one obtains:

$$|E^{Car}_{recy,sym}|^2 = \rho^2_{res}(1-L_{PRC})|\sin(2kl_-)|^2_{recy}\left(\frac{t_{PR}}{1-r_{PR}\rho_{res}\sqrt{1-L_{PRC}}[\sin(2kl_-)]_{recy}}\right)^2|E_1|^2, \tag{28}$$

$$\begin{aligned}|E^{Sid}_{recy,sym}|^2 = (1-L_{PRC})&\left|\sin\left(2kl_- \pm \frac{\Omega\Delta L}{c}\right)\right|^2_{recy} \times \\ &\times\left(\frac{t_{PR}}{1-r_{PR}\sqrt{1-L_{PRC}}[\sin\left(2kl_- \pm \frac{\Omega\Delta L}{c}\right)]_{recy}}\right)^2|E_1|^2.\end{aligned} \tag{29}$$

Since $L_{PRC} << 1$ [1], the previous equations eqs. 28-29 can be approximated as:

$$|E^{Car}_{recy,sym}|^2 = \rho^2_{res}|\sin(2kl_-)|^2_{recy}\left(\frac{t_{PR}}{1-r_{PR}\rho_{res}\sqrt{1-L_{PRC}}[\sin(2kl_-)]_{recy}}\right)^2|E_1|^2, \tag{30}$$

$$|E^{Sid}_{recy,sym}|^2 = \left|\sin\left(2kl_- \pm \frac{\Omega\Delta L}{c}\right)\right|^2_{recy}\left(\frac{t_{PR}}{1-r_{PR}\sqrt{1-L_{PRC}}[\sin(2kl_- \pm \frac{\Omega\Delta L}{c})]_{recy}}\right)^2|E_1|^2. \tag{31}$$

[1] In Advanced Virgo $L_{PRC} \sim 1500$ ppm

3 Evaluation of the recycling cavity gain for a power-recycled interferometer

Typically the recycling cavity gain is measured starting from the ratio between the power circulating in the interferometer when it is in recycled and recombined configurations.
Using eqs. 30-31 for the recycled state and eqs. 22-23 for the recombined configuration one obtains:

$$\begin{aligned}\frac{P^{Car}_{sym,recy}}{P^{Car}_{sym,rec}} = \frac{|E^{Car}_{sym,recy}|^2}{|E^{Car}_{sym,rec}|^2} = \frac{R^{Car}_{sym,recy}}{T_{PR}R^{Car}_{sym,rec}}\left(\frac{t_{PR}}{1-r_{PR}\rho_{res}\sqrt{1-L_{PRC}}[\sin(2kl_-)]_{recy}}\right)^2 = \\ = \frac{R^{Car}_{sym,recy}}{T_{PR}R^{Car}_{sym,rec}}G^{Car},\end{aligned} \tag{32}$$

$$\begin{aligned}\frac{P^{Sid}_{sym,recy}}{P^{Sid}_{sym,rec}} = \frac{|E^{Sid}_{sym,recy}|^2}{|E^{Sid}_{sym,rec}|^2} = \frac{R^{Sid}_{sym,recy}}{T_{PR}R^{Sid}_{sym,rec}}\left(\frac{t_{PR}}{1-r_{PR}\sqrt{1-L_{PRC}}[\sin(2kl_- \pm \frac{\Omega\Delta L}{c})]_{recy}}\right)^2 = \\ = \frac{R^{Sid}_{sym,recy}}{T_{PR}R^{Sid}_{sym,rec}}G^{Sid}.\end{aligned} \tag{33}$$

where $G^{Car} = \left(\frac{t_{PR}}{1-r_{PR}\rho_{res}\sqrt{1-L_{PRC}}[\sin(2kl_-)]_{recy}}\right)^2$ and $G^{Sid} = \left(\frac{t_{PR}}{1-r_{PR}\sqrt{1-L_{PRC}}[\sin(2kl_- \pm \frac{\Omega\Delta L}{c})]_{recy}}\right)^2$ are the equations used to define the recycling cavity gains for the carrier and the sidebands respectively [8].
Thus:

$$G^{Car} = T_{PR}\frac{R^{Car}_{sym,rec}}{R^{Car}_{sym,recy}}\frac{P^{Car}_{sym,recy}}{P^{Car}_{sym,rec}}, \tag{34}$$

$$G^{Sid} = T_{PR}\frac{R^{Sid}_{sym,rec}}{R^{Sid}_{sym,recy}}\frac{P^{Sid}_{sym,recy}}{P^{Sid}_{sym,rec}}. \tag{35}$$

Considering the interferometer in the recombined configuration is locked at middle fringe ($MICH = 0.5$), eqs. 34-35 can be written as:

$$G^{Car} = T_{PR}\frac{R^{Car}_{sym,HF}}{R^{Car}_{sym,recy}}\frac{P^{Car}_{sym,recy}}{P^{Car}_{sym,HF}}, \tag{36}$$

$$G^{SidLow} = T_{PR}\frac{R^{SidLow}_{sym,HF}}{R^{Sid}_{sym,recy}}\frac{P^{Sid}_{sym,recy}}{P^{Sid}_{sym,HF}}, \tag{37}$$

$$G^{SidUp} = T_{PR}\frac{R^{SidUp}_{sym,HF}}{R^{Sid}_{sym,recy}}\frac{P^{Sid}_{sym,recy}}{P^{Sid}_{sym,HF}}. \tag{38}$$

By replacing $MICH = 0.5$ in eqs. 17-18-19, the Michelson reflectivities for $\Omega = 2 \times \pi \times 6.270777$ MHz [6] are:

$$R^{Car}_{sym,HF} = 0.49, \tag{39}$$
$$R^{SidLow}_{sym,HF} = 0.47, \tag{40}$$
$$R^{SidUp}_{sym,HF} = 0.53, \tag{41}$$

for the carrier, the lower sideband and the upper one respectively.
But the gain equations are not complete since the *Frontal Modulation Technique* has to be considered to obtain the final ones.
The incoming beam (E_{in}) at frequency ω_0 is modulated at $\pm\Omega$ [2].
By modulating a signal at $\pm\Omega$ also the higher harmonics propagate in the interferometer. Considering the ideal case where the modulation at $\pm\Omega$ is perfectly sinusoidal, by applying the Jacobi-Anger expansion, the propagating electromagnetic field can be written as:

$$E = E_0 e^{i\omega_0 t}[\alpha + iae^{i\Omega t} + ibe^{-i\Omega t} + ...], \tag{42}$$

where α, a and b are constant values. Thus the power is:

$$\begin{aligned} P =& |E_0|^2[\alpha^2 + b^2 + a^2 + \\ &+ e^{i\Omega t}(ia\alpha - ib\alpha) + e^{-i\Omega t}(-ia\alpha + ib\alpha) + \\ &+ e^{i2\Omega t}(ab) + e^{-2i\Omega t}(ab) + ...]. \end{aligned} \tag{43}$$

The term $\alpha^2 + b^2 + a^2$ is the DC power, the oscillating components at $\pm\Omega$ contain the beating between the sidebands and the carrier while in $\pm 2\Omega$ components there are only the sideband contributions, i.e. they are not mixed with the carrier. Since our goal is to evaluate the sideband recycling cavity gain, in the following calculations the harmonics higher than $\pm 2\Omega$ are not considered since they don't contribute to the $\pm 2\Omega$ components.
Taking into account all these aspects, in the recombined configuration at half fringe (HF), by applying the Jacobi-Anger expansion, the field reflected by the interferometer toward the symmetric port can be written as [2]:

$$\begin{aligned} E_{rec,HF} =& E_0 e^{i\omega_0 t} t_{PR} \times [r^{Car}_{sym,HF} J_0(m_{rec}) + ir^{SidUp}_{sym,HF} J_1(m_{rec}) e^{i\Omega t} + ir^{SidLow}_{sym,HF} J_1(m_{rec}) e^{-i\Omega t} - \\ &- r^{SidUp}_{sym,HF} J_2(m_{rec}) e^{i2\Omega t} - r^{SidLow}_{sym,HF} J_2(m_{rec}) e^{-i2\Omega t}], \end{aligned} \tag{44}$$

where the $J_n(m_{rec})$ are the Bessel functions of n order and m_{rec} is the modulation index adopted in the recombined configuration. Different reflection coefficients have been used for carrier and sidebands (eqs. 12-13), respectively.

By multiplying $E_{rec,HF}$ with its complex conjugate one obtains:

$$\begin{aligned}
P_{rec,HF} =& P_0 T_{PR}\Big\{ R^{Car}_{sym,HF} J_0^2(m_{rec}) + R^{SidUp}_{sym,HF} J_1^2(m_{rec}) + R^{SidLow}_{sym,HF} J_1^2(m_{rec}) + \\
&+ R^{SidUp}_{sym,HF} J_2^2(m_{rec}) + R^{SidLow}_{sym,HF} J_2^2(m_{rec}) + \\
&+ e^{-i\Omega t}\Big[J_0(m_{rec}) J_1(m_{rec}) \Big(-i r^{Car}_{sym,HF} r^{SidUp*}_{sym,HF} + i r^{Car*}_{sym,HF} r^{SidLow}_{sym,HF} \Big) - \\
&- J_1(m_{rec}) J_2(m_{rec}) \Big(i R^{SidLow}_{sym,HF} - i R^{SidUp}_{sym,HF} \Big) \Big] + \\
&+ e^{i\Omega t}\Big[J_0(m_{rec}) J_1(m_{rec}) \Big(i r^{Car*}_{sym,HF} r^{SidUp}_{sym,HF} - i r^{Car}_{sym,HF} r^{SidLow*}_{sym,HF} \Big) + \\
&+ J_1(m_{rec}) J_2(m_{rec}) \Big(i R^{SidUp}_{sym,HF} - i R^{SidLow}_{sym,HF} \Big) \Big] + \\
&+ e^{i2\Omega t}\Big[J_1^2(m_{rec}) r^{SidUp}_{sym,HF} r^{SidLow*}_{sym,HF} - \\
&- J_0(m_{rec}) J_2(m_{rec}) \Big(r^{Car*}_{sym,HF} r^{SidUp}_{sym,HF} + r^{SidLow*}_{sym,HF} r^{Car}_{sym,HF} \Big) \Big] + \\
&+ e^{-i2\Omega t}\Big[J_1^2(m_{rec}) r^{SidUp*}_{sym,HF} r^{SidLow}_{sym,HF} - \\
&- J_0(m_{rec}) J_2(m_{rec}) \Big(r^{Car}_{sym,HF} r^{SidUp*}_{sym,HF} + r^{SidLow}_{sym,HF} r^{Car*}_{sym,HF} \Big) \Big] \Big\},
\end{aligned} \tag{45}$$

so the signal at $\pm 2\Omega$ is:

$$P^{2\Omega}_{rec,HF} = P_0 T_{PR}\Big[2 J_1^2(m_{rec}) \sqrt{R^{SidUp}_{sym,HF}} \sqrt{R^{SidLow}_{sym,HF}} + 2 J_0(m_{rec}) J_2(m_{rec}) \sqrt{R^{Car}_{sym,HF}} \Big(\sqrt{R^{SidUp}_{sym,HF}} + \sqrt{R^{SidLow}_{sym,HF}} \Big) \Big], \tag{46}$$

having replaced $r^{Car}_{sym,HF}$, $r^{SidUp}_{sym,HF}$ and $r^{SidLow}_{sym,HF}$ with eqs. 12-13 [2].

In the recycled configuration the $\pm 2\Omega$ fields are suppressed because of the power recycling cavity is resonant only for the carrier and the sideband at $\pm\Omega$, thus the field circulating in the interferometer is:

$$\begin{aligned}
E_{recy} =& E_0 e^{i\omega_0 t} \times [\sqrt{G^{Car}} r^{Car}_{sym,recy} J_0(m_{recy}) + i\sqrt{G^{Sid}} r^{SidUp}_{sym,recy} J_1(m_{recy}) e^{i\Omega t} + \\
&+ i\sqrt{G^{Sid}} r^{SidLow}_{sym,recy} J_1(m_{recy}) e^{-i\Omega t}].
\end{aligned} \tag{47}$$

[2] Note that the phase term in eq. 13, i.e. $e^{\pm \frac{i2\Omega}{c} l_+}$ is negligible with respect to the other phase term in the same equation, i.e. e^{2ikl_+}, since f_{mod} is 6 MHz with respect to the main laser frequency f_{laser} that is 282 THz. This consideration is also valid for the other modulation frequencies reported in Tab. 1.

By multiplying E_{recy} with its conjugate complex one obtains:

$$\begin{aligned}P_{recy} =& P_0\Big\{R^{Car}_{sym,recy}J_0^2(m_{recy}) + G^{Sid}R^{SidUp}_{sym,recy}J_1^2(m_{recy}) + G^{Sid}R^{SidLow}_{sym,recy}J_1^2(m_{recy}) + \\ &+ e^{i\Omega t}\left[iJ_0(m_{recy})J_1(m_{recy})\sqrt{G^{car}}\sqrt{G^{Sid}}\left(r^{Car*}_{sym,recy}r^{SidUp}_{sym,recy} - r^{Car}_{sym,recy}r^{SidLow*}_{sym,recy}\right)\right] + \\ &+ e^{-i\Omega t}\left[iJ_0(m_{recy})J_1(m_{recy})\sqrt{G^{car}}\sqrt{G^{Sid}}\left(r^{Car*}_{sym,recy}r^{SidLow}_{sym,recy} - r^{Car}_{sym,recy}r^{SidUp*}_{sym,recy}\right)\right] + \\ &+ e^{2i\Omega t}\left[r^{SidUp}_{sym,recy}r^{SidLow*}_{sym,recy}G^{Sid}J_1^2(m_{recy})\right] + \\ &+ e^{-2i\Omega t}\left[r^{SidUp*}_{sym,recy}r^{SidLow}_{sym,recy}G^{Sid}J_1^2(m_{recy})\right]\Big\}.\end{aligned} \tag{48}$$

Thus the signal at $\pm 2\Omega$ is:

$$P^{2\Omega}_{recy} = P_0 2J_1^2(m_{recy})\sqrt{R^{SidUp}_{sym,recy}}\sqrt{R^{SidLow}_{sym,recy}}G^{Sid}. \tag{49}$$

The sideband recycling cavity gain is given by the ratio between eq. 49 and eq. 46:

$$\begin{aligned}G^{Sid} =& T_{PR}\frac{P^{2\Omega}_{recy}}{P^{2\Omega}_{rec}}\times \\ &\times\frac{\left[2J_1^2(m_{rec})\sqrt{R^{SidUp}_{sym,HF}}\sqrt{R^{SidLow}_{sym,HF}} + 2J_0(m_{rec})J_2(m_{rec})\sqrt{R^{Car}_{sym,HF}}\left(\sqrt{R^{SidUp}_{sym,HF}} + \sqrt{R^{SidLow}_{sym,HF}}\right)\right]}{2J_1^2(m_{recy})\sqrt{R^{SidUp}_{sym,recy}}\sqrt{R^{SidLow}_{sym,recy}}} = \\ &= T_{PR}\frac{P^{2\Omega}_{recy}}{P^{2\Omega}_{rec}}B,\end{aligned} \tag{50}$$

where

$$B = \frac{\left[2J_1^2(m_{rec})\sqrt{R^{SidUp}_{sym,HF}}\sqrt{R^{SidLow}_{sym,HF}} + 2J_0(m_{rec})J_2(m_{rec})\sqrt{R^{Car}_{sym,HF}}\left(\sqrt{R^{SidUp}_{sym,HF}} + \sqrt{R^{SidLow}_{sym,HF}}\right)\right]}{2J_1^2(m_{recy})\sqrt{R^{SidUp}_{sym,recy}}\sqrt{R^{SidLow}_{sym,recy}}}. \tag{51}$$

Given that:

$$\sqrt{R^{SidLow}_{sym,HF}} \sim \sqrt{R^{SidUp}_{sym,HF}} \sim \sqrt{R^{Car}_{sym,HF}} = \sqrt{R_{sym,HF}} \tag{52}$$

$$\sqrt{R^{SidUp}_{sym,recy}} \sim \sqrt{R^{SidLow}_{sym,recy}} = \sqrt{R^{Sid}_{sym,recy}}, \tag{53}$$

eq. 50 can be written as:

$$\begin{aligned}G^{Sid} =& T_{PR}\frac{P^{2\Omega}_{recy}}{P^{2\Omega}_{rec}}\frac{R_{sym,HF}}{R^{Sid}_{sym,rec}}\frac{[2J_1(m_{rec})^2 + 4J_0(m_{rec})J_2(m_{rec})]}{2J_1^2(m_{recy})} = \\ &= T_{PR}\frac{P^{2\Omega}_{recy}}{P^{2\Omega}_{rec}}A,\end{aligned} \tag{54}$$

where

$$A = \frac{R_{sym,HF}}{R^{Sid}_{sym,recy}} \frac{[2J_1^2(m_{rec}) + 4J_0(m_{rec})J_2(m_{rec})]}{2J_1^2(m_{recy})}. \tag{55}$$

At the dark fringe A and B converge to the same value and if $m_{recy} = m_{rec} = m$, A and B converge to 1, as it is shown in Fig. 5.

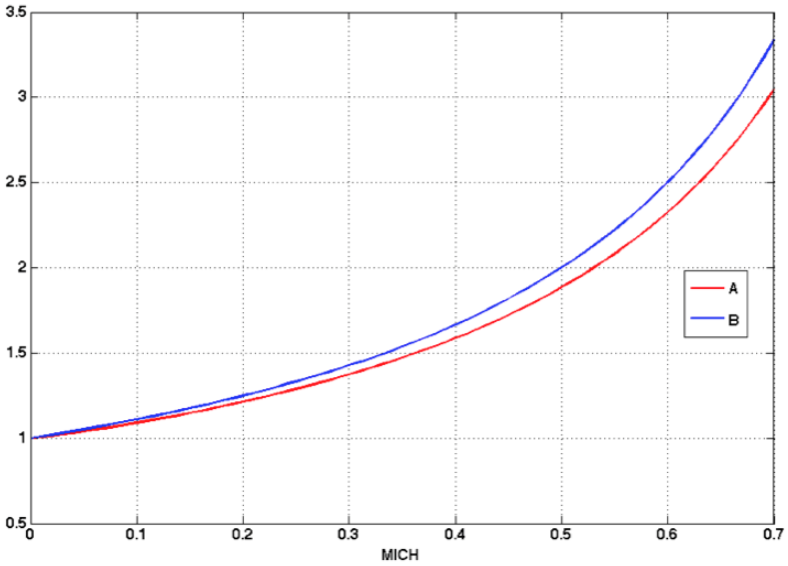

Figure 5: *Evolution of A and B when $m_{rec} = m_{recy} = m$ during the lock acquistion sequence.*

Thus at the dark fringe eq. 54 is a good approximation of eq. 50 and if $m_{recy} = m_{rec} = m$, i.e. $A = 1$, the recycling cavity gain on the symmetric port can be evaluated as:

$$G^{Sid}_{B4} = T_{PR} \frac{P^{2\Omega}_{recy}}{P^{2\Omega}_{rec}}, \tag{56}$$

where $B4$ indicates the photodiode located on the symmetric port in Advanced Virgo (Fig. 6).

It is also useful to notice that when $m_{recy} = m_{rec} = m$ the *pdh* term defined as:

$$pdh = \frac{[2J_1(m)^2 + 4J_0(m)J_2(m)]}{2J_1(m)^2}, \tag{57}$$

is approximately 2 independently from the modulation index value m (Fig. 7).

In Virgo the photodiode used to measure the sideband recycling cavity gain was $B5$ whose positioning is shown in Fig. 6 [8]. In this case only the beam reflected by the NI Fabry-Pérot cavity impinges on the photodiode thus, the reflectivity of the Michelson interferometer is not involved in the gain measurement.
The reflectivity to be considered is that of the Fabry-Pérot cavity $R_{anti} = r^2_{anti} = -1$ (eq. 2), that it does not change during the entire lock acquisition sequence, i.e. from recombined to recycled state.
Thus from eq. 54:

$$G^{Sid}_{B5} = T_{PR} \frac{P^{2\Omega}_{rec}}{P^{2\Omega}_{rec}} \frac{[2J_1(m_{rec})^2 + 4J_0(m_{rec})J_2(m_{rec})]}{2J_1^2(m_{recy})}, \tag{58}$$

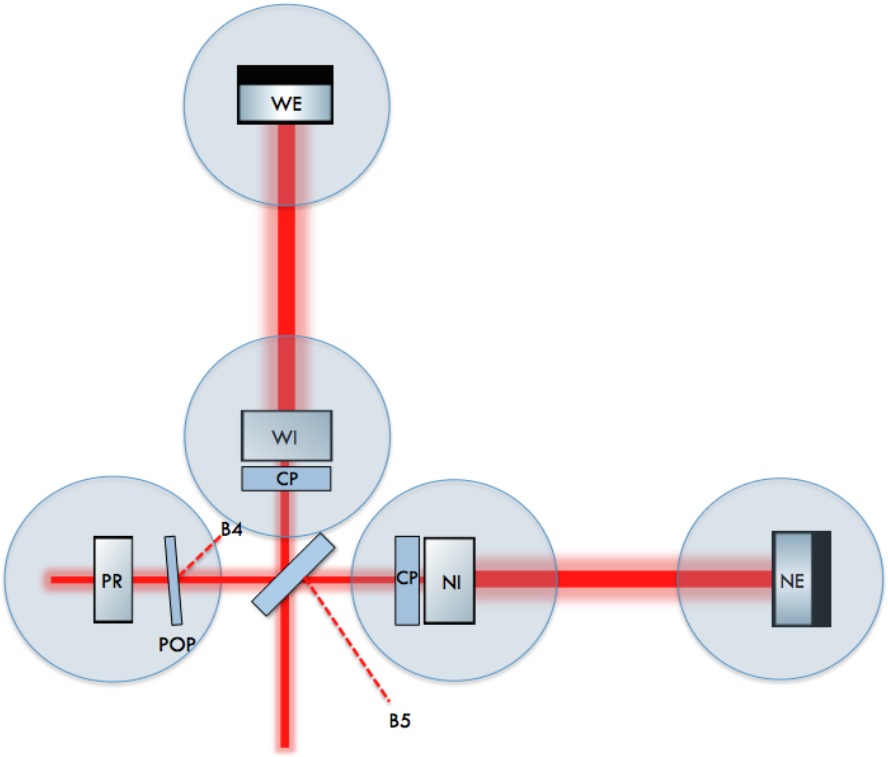

Figure 6: *Photodiodes B4 and B5 in the interferometer. The pick off plate (POP) used to extract the B4 pick off beam is also shown [6].*

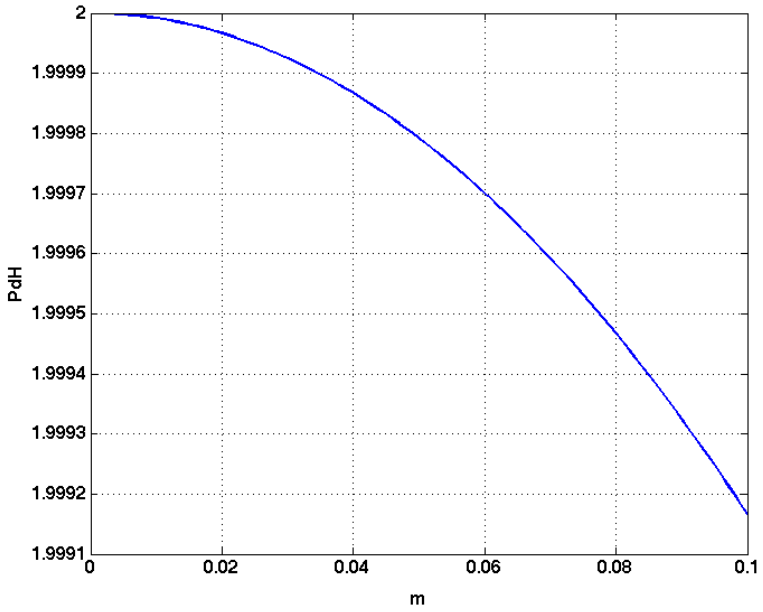

Figure 7: *The behaviour of pdh factor when $m_{rec} = m_{recy} = m$ changing m of two orders of magnitude.*

and when $m_{recy} = m_{rec} = m$ the above equation becomes:

$$G_{B5}^{Sid} = T_{PR} \frac{P_{recy}^{2\Omega}}{P_{rec}^{2\Omega}} 2, \tag{59}$$

that can be applied to evaluate the recycling cavity gain by the signal at 2Ω of the $B5$ photodiode.

In the next section the reliability of the model will be checked using the 6 MHz sidebands, but the equations derived in this note can be applied to evaluate the recycling cavity gain for all modulation frequencies summarized in Tab. 1.

4 6 MHz G_{rec} measurement from ITF data

To check the consistency between $B4$ and $B5$ the data set referred to a stable dark fringe lock during the first engineering run of Advanced Virgo at $GPS = 1178065308$ has been analyzed. The decrease of the 6 MHz modulation depth to prevent the B4 from saturating during the lock acquisition sequence has also been considered [9], i.e.:

$$m_{rec} = 0.2 \quad \text{and} \quad m_{recy} = 0.036, \tag{60}$$

for the recombined and recycled at dark fringe configurations respectively. Thus the pdh term becomes:

$$pdh = \frac{[2J_1(m_{rec})^2 + 4J_0(m_{rec})J_2(m_{rec})]}{2J_1(m_{recy})^2} = 61.72. \tag{61}$$

Thus for $B4$ (eq. 54) and $B5$ (eq. 58) are valid:

$$G_{B4}^{Sid} = T_{PR} \frac{P_{recy}^{2\Omega}}{P_{rec}^{2\Omega}} \frac{R_{sym,HF}}{R_{sym,recy}^{Sid}} 61.72, \tag{62}$$

and

$$G_{B5}^{Sid} = T_{PR} \frac{P_{recy}^{2\Omega}}{P_{rec}^{2\Omega}} 61.72. \tag{63}$$

The recycling gain for the 6 MHz sidebands extracted from $B4$ and $B5$ signals at 12 MHz are consistent (Fig. 8).

This is confirmed by the histograms of the two data sets (Fig. 9) where the peaks of the distributions are both around $G^{Sid} \sim 30$ consistent with the results from optical simulations [10, 11]. The recycling cavity gain varies in the range 15-50. This behaviour, at present under investigation, is probably due to alignement fluctuations.

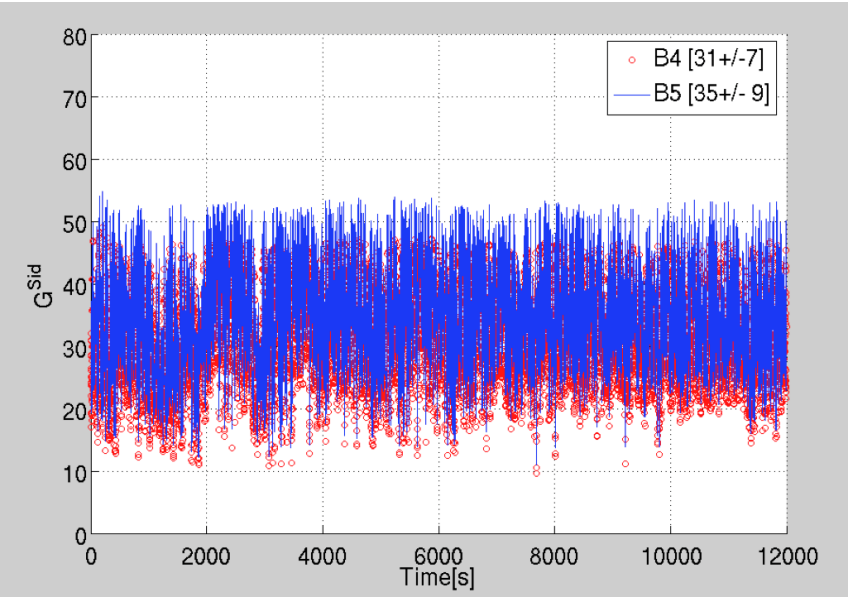

Figure 8: *The cavity recycling gains measured by B4 and B5 for the lock at GPS* = 1178065308.

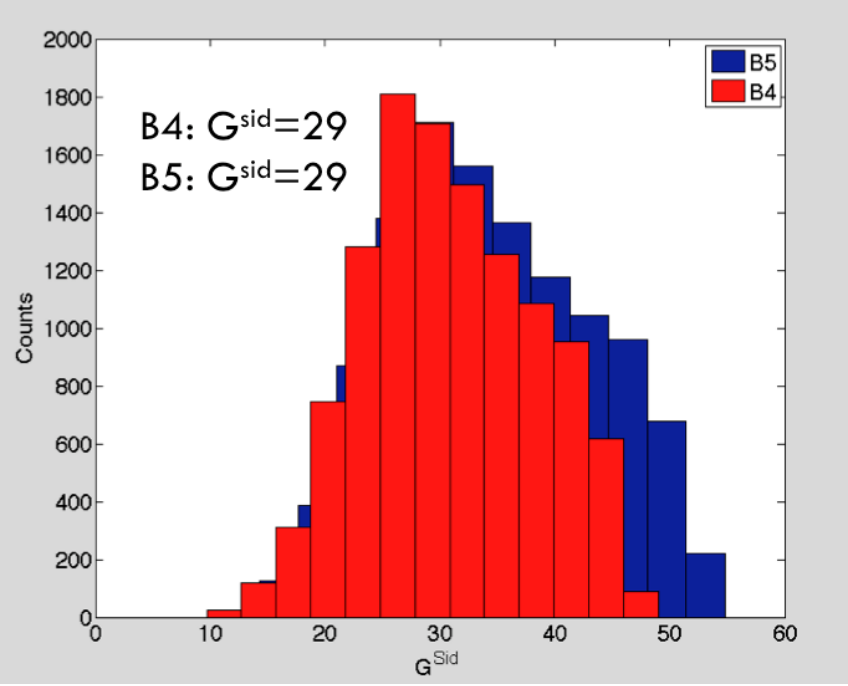

Figure 9: *The histograms of the cavity recycling gains measured by B4 and B5 for the lock at GPS* = 11178065308.

5 Conclusions

In this document a model to evaluate the sideband recycling cavity gain has been derived describing the main fields propagation in the resonant Fabry-Pérot cavity, the recombined and the power recycled Michelson interferometer. The calculations have been developed for the symmetric port of the detector providing the equation to evaluate the sideband gain from $B4$ photodiode taking also into account the *Frontal Modulation Technique*. Through simple adjustments of the model the formula to evaluate the sideband gain from the $B5$ photodiode has been also defined. In the last part the models have been applied to a set of data for a dark fringe lock of AdV. The 6 MHz sidebands gains evaluated by both photodiodes are consistent and in agreement with results from optical simulations, confirming the reliability of the model.

6 Acknowledgments

I thank Gabriele Vajente for his overseas help, the TCS Group for the useful discussions and Matteo Barsuglia for all his expert advice.

References

[1] G. Vajente, *Signal Recycling I: Field equations*, VIR-030B-08, (2008). 3, 5, 7

[2] L. Matone, Ètude du controle global de l'interferometer central de Virgo, Ph.D. Thesis, Université de Paris-Sud, (1999). 3, 10

[3] L. Pinard, *Power Recycling Mirror characterization*, VIR-0029A-15, (2015). 4

[4] G. Vajente , *VESF School on Advanced Gravitational Wave Detectors*, (2012). 4

[5] J. Degallaix, Communication in the Advanced Virgo Optics Mailing List, (2017). 6

[6] The Virgo Collaboration, *Advanced Virgo Baseline Design*, VIR-27A-09, (2009). 4, 6, 10, 14

[7] M. Barsuglia, P. Ruggi, D. Hoak, *Locking shift: new MICH error signal* ($B1p/B1p+B4$), *loop measurements, some progress with* 10 *Hz oscillations*, Virgo logbook entry 36117, (2017). 6

[8] L. Barsotti, *The control of the Virgo interferometer for gravitational wave detection*, Ph.D. Thesis, Univerisità degli Studi di Pisa, (2006). 9, 13

[9] F. Berni, D. Bersanetti, V. Boschi, F. Carbognani, D. Hoak, M. Mantovani, G. Pillant, P. Ruggi, B. Swinkels, M. Was, 6 *MHz modulation depth reduced*, Virgo logbook entry 37275, (2017). 15

[10] J. Degallaix, M. Pichot, A. Rocchi, *Update on simulation crosschecks*, VIR-0136A-17, (2017). 15

[11] H. Yamamoto, *Analysis of marginally stable cavity of AdVirgo*, LIGO-G1700709, (2017). 15